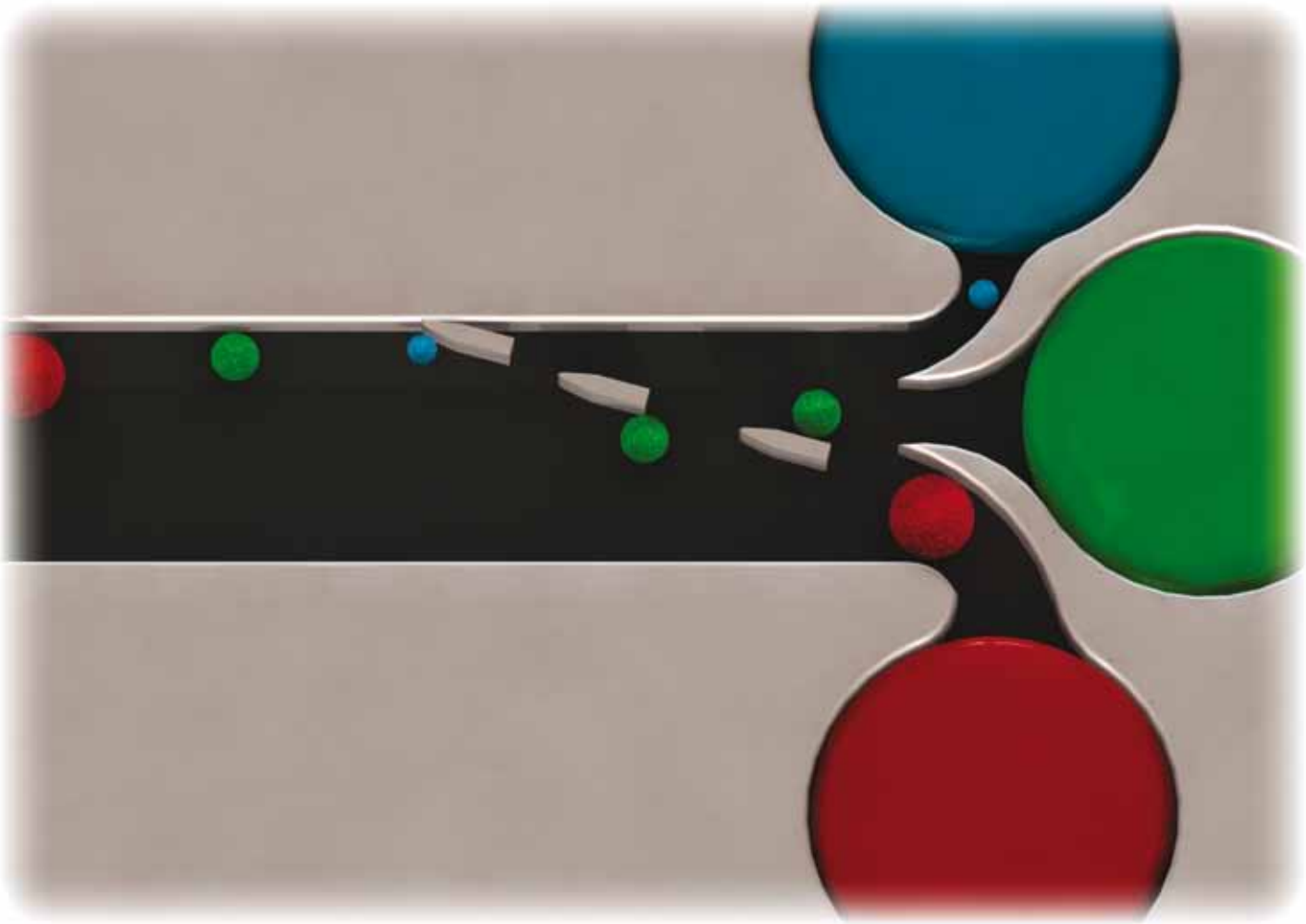

**Featuring research from the Microsystems Laboratory of Dr Chih-Ming Ho in the Mechanical and Aerospace Engineering Department at the University of California, Los Angeles.**

**Title: Continuous sorting of heterogeneous-sized embryoid bodies**

Embryoid bodies (EBs) are spherical aggregates of spontaneously differentiating embryonic stem cells and EB-mediated differentiation efficiency is critically dependent upon EB size. This paper presents a microfluidic device for sorting EBs into multiple size-dependent groups with high separation efficiencies. Our proposed separation scheme utilizes appropriated spaced pillars within a microchannel to alter the fluid flow pathway, thus allowing particles of defined sizes to be diverted into size-specific collection reservoirs.

**As featured in:**

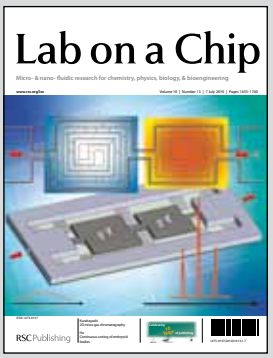


See Ho *et al.*, *Lab Chip*, 2010, **10**, 1678–1682

# Continuous sorting of heterogeneous-sized embryoid bodies†

Peter B. Lillehoj,[a] Hideaki Tsutsui,[a] Bahram Valamehr,[b] Hong Wu[b] and Chih-Ming Ho*[a]

*Received 5th January 2010, Accepted 12th March 2010*
*First published as an Advance Article on the web 7th April 2010*
**DOI: 10.1039/c000163e**



This paper presents a microfluidic device for sorting embryoid bodies (EBs) with large dynamic size ranges up to 300 μm. The proposed separation scheme utilizes appropriately spaced pillars within a microchannel to alter the fluid flow pathway, thus allowing particles of defined sizes to be diverted towards specific flow paths. We test the device functionality by separating polystyrene beads 90, 175 and 275 μm in diameter, demonstrating separation efficiencies approaching 100%. We then demonstrate for the first time on-chip separation of mouse EBs, which were separated into three size groups. The ability to extract specific size ranges of EBs will greatly facilitate their subsequent differentiation studies.

## Introduction

With their developmental potential to differentiate into all three of the germ layers (endoderm, mesoderm and ectoderm), embryonic stem (ES) cells provide a unique opportunity to study lineage commitment and can potentially serve as a source of specialized cells for regenerative medicine. Among the various published ES cell differentiation protocols,[1–4] the formation of embryoid bodies (EBs), spherical aggregates of spontaneously differentiating ES cells, is commonly utilized as a critical intermediate step. EBs appear to recapitulate embryonic development, facilitating induction of differentiation and commitment into specific cell types.[5] There are several conventional methods to create EBs *in vitro*, including suspension culture on low-attachment plates and hanging drop methods; however, these methods suffer from heterogeneous size distribution or lack of scalability.[6] We recently reported that EB-mediated differentiation efficiency is critically dependent upon EB size. EBs between 100 and 300 μm in diameter had the highest survival rate and greatest expression of genetic markers of differentiation.[7,8] Therefore, obtaining EBs of homogeneous size appears to be a key factor for successful ES cell research.

Microfluidic processes can be an efficient means for the separation/sorting of particles and biological cells. To date, numerous techniques have been developed to separate micron-sized samples including those utilizing acoustic, magnetic, optical, or electric forces.[9–12] Although these techniques allow for continuous separation on a miniaturized platform, they require the use of external force fields. Methods based on gravitational[13] and centrifugal forces[14] have also been demonstrated; however, these require long processing times or bulky external devices. Alternatively, work has been done to create microdevices based on fluorescence (μFACS).[15,16] Some of these techniques require particle/cellular modification prior to separation, thereby incurring particle damage and complicated sample collection procedures. To circumvent these problems, researchers have been developing separation techniques based solely on particle size and fluidic forces within a microchannel. This strategy offers improved specimen integrity while simplifying sample preparation procedures for lab-on-a-chip biological/chemical analysis. Furthermore, by integrating this technique onto a compact microfluidic platform, additional advantages of lower production costs and reduced reagent consumption are achieved.

Recent research on flow-based separators has led to several techniques, including deterministic lateral displacement,[17,18] pinched flow fractionation (PFF),[19,20] hydrodynamic filtration,[21] Brownian ratchet separation,[22] asymmetric cavity flow separation[23] and hydrophoretic separation.[24] These techniques can achieve continuous particle separation with high efficiencies, which is crucial for large-scale processing; however, these methods are designed for small particles and cells less than 25 μm in diameter. The present device was designed to simultaneously sort particles within a large size range (from 1–300 μm), allowing for the separation of a wide variety of samples which differ in orders of magnitude in size. Compared with smaller sized particles, the influence of inertial forces is more dominant for larger sized particles, which is an important concept to consider for their separation. Based on this device, we demonstrate the separation of mouse EBs, which vary from tens to hundreds of microns in size.

Current pipetting methods for separating EBs are time consuming, inefficient and result in poor size uniformity. Additionally, the separation of EBs through external force fields, such as dielectrophoretic (DEP), acoustic or magnetic, may raise potential issues in damaging the fragile cellular entities, thereby affecting subsequent cell differentiation. Replacing low-attachment plates with hydrophobic surfaces, such as polydimethylsiloxane (PDMS), can significantly improve homogeneity of the EB size.[7] Alternatively, several research groups employed microdevices, such as microwells[25] and microchannel compartments,[26] to physically define the size of

[a]*Mechanical and Aerospace Engineering Department, University of California, Los Angeles, CA, USA. E-mail: chihming@seas.ucla.edu; Tel: +1 310-825-9993*
[b]*Department of Molecular and Medical Pharmacology, David Geffen School of Medicine, Los Angeles, CA, USA*

† Electronic supplementary information (ESI) available: Computation modeling, materials and methods for device fabrication, EB preparation, experimental setup, EB viability analysis, COMSOL simulations for various channel configurations and data on EB viability. See DOI: 10.1039/c000163e

 

growing EBs. While these latter methods attempted to obtain homogeneous EBs by manipulating their growth conditions, our approach has been to separate a population of heterogeneous EBs into uniform size groups using a novel microfluidic sorting procedure. Continuous sorting of EBs by size can be a valuable tool for obtaining large numbers of homogeneous EBs using either conventional EB forming platforms or the newer culture methods, potentially facilitating EB-mediated differentiation of embryonic stem cells.

The proposed method of separation is solely based upon the modification of a fluid flow pathway within a microchannel through the strategic positioning and geometric design of micro-sized pillars. In this paper, computational modeling of the flow profile is presented to guide the rationale in designing the device. The separation efficiency of the device was calibrated using polystyrene beads of three different sizes. Finally, high-throughput separation of EBs is presented.

## Results and discussion

### Microchannel design

The fluidic network (Fig. 1B) was designed for high separation efficiency and high throughput while maintaining a compact profile. The particles are sorted within a narrow separation region (spanning less than ~1.3 mm) which is located immediately upstream of the outlet branches. This region is comprised of bullet-shaped pillars which are strategically placed within the channel to alter the flow pathway. The modified pathlines allow for particles to be diverted toward predetermined branches of specific size groups (0–100 μm, 100–200 μm and 200–300 μm). A sheath flow is utilized to align the particles along the upper wall of the channel prior to separation. This sheath flow produces a normal force to the channel wall to minimize the vertical displacement caused by the inertial forces of the particles.

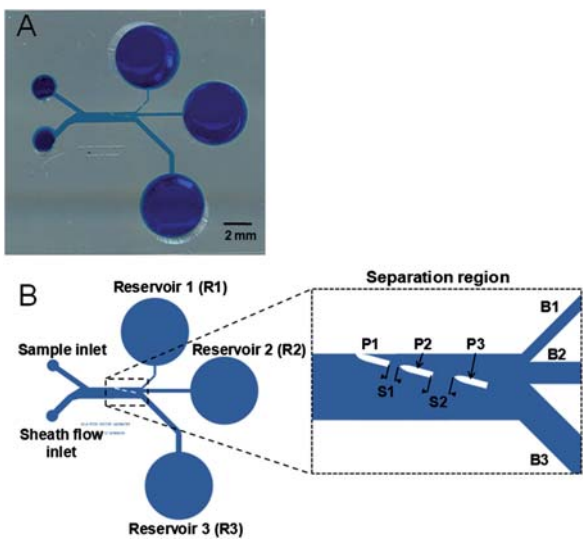


**Fig. 1** (A) Photograph of the proposed sorting device. The overall device is roughly 16 mm × 16 mm and is filled with dye for enhanced visualization of the fluidic network. (B) Schematic illustration labeling the relevant sections with an enlarged view of the separation region.

Computation simulations were performed to optimize the sheath flow for enhanced particle alignment (see Fig. S2 in ESI†).

Simulations were also performed to optimize the pillar geometry and configuration for optimal separation efficiency (see Fig. S3 and S4 in ESI†). Various parameters (*i.e.*, pillar geometry, pillar angle and inter-pillar spacing) were modified to observe their effects on the response of the system. Based on our results, the pillars are designed with lengths and widths of 300 μm and 60 μm respectively and are positioned at a 15° angle with respect to the upper channel wall. The spacing between the first and second set of pillars, S1 and S2, are 115 μm and 210 μm respectively. Pillar angles <15° had a minimal effect on altering the flow profile, resulting in closely packed pathlines unable to sufficiently divert particles to their corresponding outlets. However, angles ≫15° dramatically obstructed the flow profile, which would cause particles to veer off their intended pathlines. In terms of pillar configuration, inter-pillar spaces much larger than their corresponding particle size would allow for the passage of smaller particles, thus lowering the separation efficiency.

The width of the main channel is 640 μm and the widths of the upper (B1), middle (B2) and lower (B3) outlet branches are 120 μm, 220 μm, and 320 μm respectively. The height of all the channels is 340 μm. The widths of the outlet branches are designed not only to minimize particle clogging, but also to correspond with the spacing between the respective pillars so as to maximize the flow of the particles into their respective reservoirs. The reservoirs are 4 mm in diameter and are open to the atmosphere which allows for the sorted particles to be easily collected using a pipette. The overall size of the PDMS chip is 16 mm × 16 mm (Fig. 1A), which greatly minimizes the footprint of this system and enables for large batch fabrication.

### Separation of polystyrene beads

Initial experiments were performed to separate polystyrene beads into 0–100 μm, 100–200 μm and 200–300 μm groups. The flow rates of the sample and buffer solutions were adjusted to align the particles along the upper wall of the channel. Essentially, the flow rates were modified to produce an optimal velocity shear, in which the force normal to the particle path could push the particle against the upper channel wall. A flow rate of 5 μL $min^{-1}$ with a ratio of 4 : 1 (buffer : sample) was sufficient to maintain proper flow focusing. The smallest particles (≤100 μm) could be easily focused alongside the upper wall throughout the channel and could follow their corresponding pathlines. Due to the exact spacing between the pillars, these smaller particles were able to move through inter-pillar space S1 between pillars P1 and P2 and remain on the flow path leading towards branch B1 (Fig. 2A). Particles between 100 and 200 μm were also focused along the upper channel wall as they encountered the pillars; however, they were too large to enter space S1 between pillars P1 and P2. Following their corresponding pathlines, these particles flowed past P2 and entered into space S2 between pillars P2 and P3, leading towards branch B2 (Fig. 2B). Similarly, the largest particles (200–300 μm) flowed past pillar P3 and were guided toward branch B3 (Fig. 2C). By observing the simulation results of pathlines in the separation region (Fig. S1 in ESI†), it is

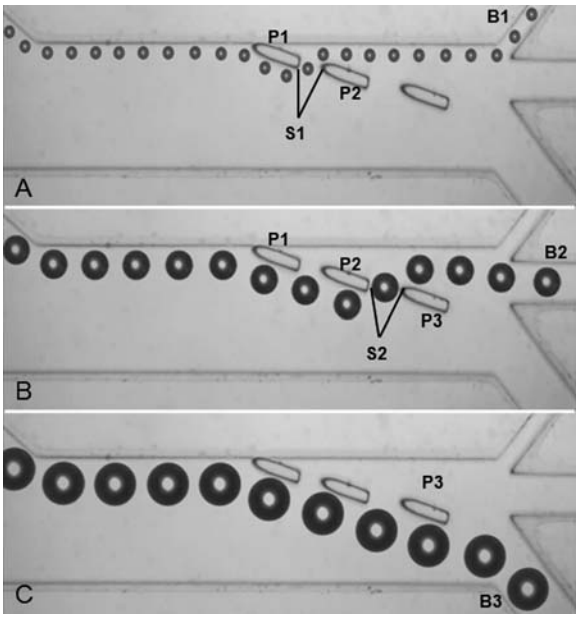


**Fig. 2** Trace of polystyrene beads showing their trajectory within the microchannel: (A) 90 μm in size, (B) 175 μm in size and (C) 275 μm in size. Images were generated by superimposing video frames.

apparent that the experimental results follow very closely with numerical simulations.

Based on this approach, only three pillars are needed for separation into three size ranges, which is a much simpler design than previous techniques. Such a simplified design greatly reduces the complexity of the system, especially for multiple size separation. Another advantage of this approach is the high separation efficiencies that are achievable. Fig. 3 shows the size distribution of particles in each reservoir for the sorting of a mixed population of particles. Reservoirs R1 (0–100 μm), R2 (100–200 μm) and R3 (200–300 μm) exhibited purities of 100%, 92% and 92% respectively based on a population of several hundred particles. The careful design of the separation region, *i.e.*, the precise spacing between the pillars and specific channel dimensions, enables for such high separation specificity to be achieved. Additionally, the 100% purity of particles in Reservoir

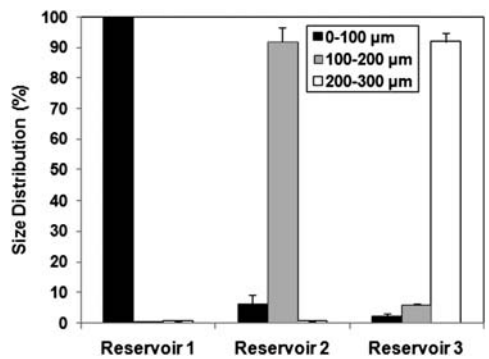


**Fig. 3** Size distribution of particles in each of the three reservoirs. Experiments were performed at a flow rate of 5 μL $min^{-1}$. Error bars represent the standard deviation of sorted beads from several independent experiments.

R1 is due to larger particles being unable to enter the upper branch. Generally, while larger particles were unable to enter reservoirs intended for smaller particles, it was possible for smaller particles to enter incorrect reservoirs, which is evident by the lower purities of Reservoirs R2 and R3. However, particles will enter their respective reservoirs if they are properly focused prior to entering the separation region. Based on this principal, we determined that the separation efficiency is greatly affected by the quality of particle focusing and the ability of the particles, particularly smaller ones, to remain in their intended pathlines. By operating in the microscale regime, this can be achieved by maintaining laminar flow and precisely controlling the experimental flow rates.

In addition to proper particle focusing, the distribution of particles within the microchannel is another important factor that was observed to affect the operation of the device. Sample solutions with high particle concentrations tended to form particle clusters that occluded the inter-pillar spaces, thus inhibiting separation. Clumped particles were also poorly focused, causing them to veer outside of their intended pathlines and flow toward an incorrect reservoir. Additionally, grouped particles will naturally follow unique pathlines since their centroids have been altered. To account for these issues, beads were diluted to a concentration of approximately $10^3$ beads per mL during sample preparation. Sample dilution ensured that particles were adequately spaced within the microchannel to minimize particle clustering and alleviate device clogging. However, excessive sample dilution reduced device throughput. In order to address this concern, experiments were performed at higher flow velocities to increase the sorting rate. Increasing the flow rate to 20 μL $min^{-1}$ did not significantly affect separation efficiency. At this flow rate, the beads could be separated at a rate of 5 $s^{-1}$.

## Separation of EBs

The results from EB separation experiments matched very closely with those from the bead experiments. EBs could be properly focused utilizing a flow rate ratio of 4 : 1 (buffer : sample) and maintained their streamline positions within the microchannel. As previously mentioned, the proposed separation scheme enables for simultaneous separation, in which specimens of different sizes can be processed in a concurrent manner. Shown in Fig. 4 is the simultaneous sorting of three mouse EBs of 90, 160 and 300 μm in diameter. Similar to the separation of polystyrene beads, high separation efficiencies could also be achieved with EBs (Fig. 5). Reservoirs 1 (0–100 μm), 2 (100–200 μm) and 3 (200–300 μm) exhibited purities of 100%, 86% and 81% respectively based on a population of several hundred EBs. The effects of flow rate on EB separation were also studied and it was found that altering the flow rates did not have a negative impact on the separation efficiency. However, flow velocities >20 μL $min^{-1}$ damaged the EBs, causing them to break apart. Unlike polystyrene beads, EBs are comprised of individual ES cells packed together in a spherical mass and high flow velocities were detrimental to their structure. An operational flow rate ≤16 μL $min^{-1}$ ensured EB integrity, preventing cell disassociation.

To evaluate the effects of the proposed microfluidic separation technique on cell viability, a flow cytometry analysis was

 

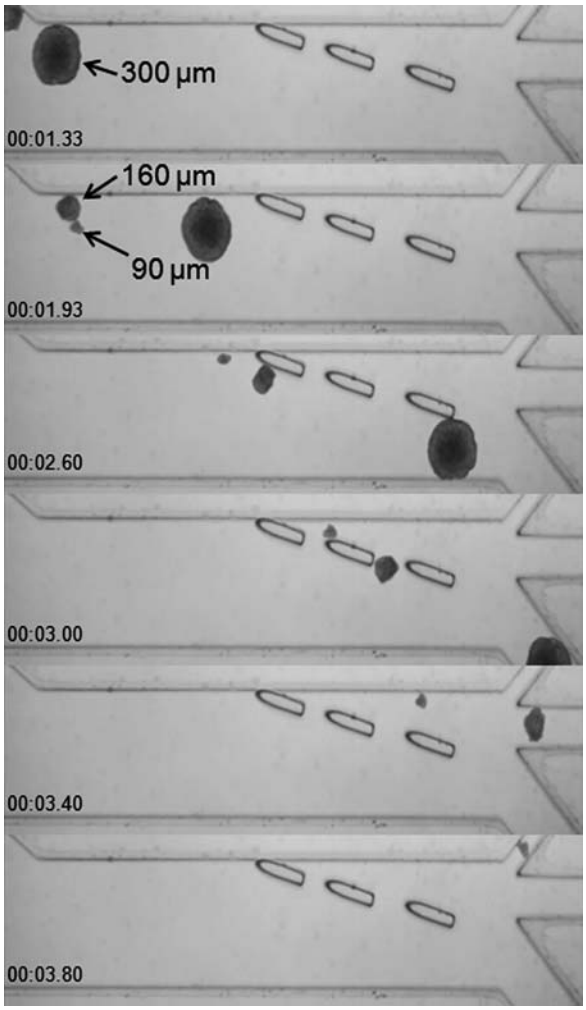


**Fig. 4** Sequential video frames demonstrating the simultaneous separation of mouse EBs 90, 160 and 300 μm in size. This experiment was performed at a flow rate of 5 μL $min^{-1}$. Time stamps are located at the bottom left corners of each frame.

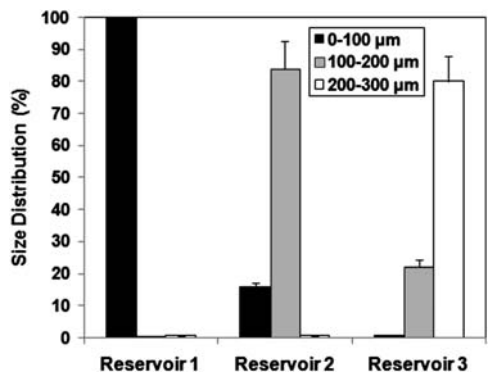


**Fig. 5** Size distribution of EBs in each of the three reservoirs. The results are based on continuous cell separation, excluding clogging events. Experiments were performed at a flow rate of 5 μL $min^{-1}$. Error bars represent the standard deviation of sorted EBs from several independent experiments.

conducted on both sorted and control (unsorted) EB populations. Cell viability, measured by the percentage of a population negative to 7-AAD staining, showed minimal and temporal impacts on cell viability (see Fig. S5 in ESI†). The issue of clogging that was observed during bead experiments was more prevalent during EB separation. EBs exhibited a higher degree of clustering than beads, even at low cell concentrations. Additionally, current methods for EB formation lack size and shape controllability, resulting in nonspherical-shaped cell formations. As previously mentioned, specimen uniformity plays a crucial role in the proper operation of this device. EBs heterogeneous in shape were likely to shift toward different pathlines or obstruct the device. As a result, the separation efficiencies for EB experiments were slightly lower compared with bead experiments. While it is not required for EBs to be perfectly spherical in shape, it is important that they maintain a certain degree of homogeneity to follow the separation principals of the device. The ability to form homogenous EBs is possible through the study of their growth and formation procedures.[25,26,27]

## Conclusions

A microfluidic device capable of separating EBs and polystyrene beads is presented. The unique design employed in this device allows for separation into size-dependent groups with a high degree of uniformity. Compared with conventional microfluidic devices employing similar separation principals, this method enables for continuous separation of large particles and cells (≤300 μm) in a compact device, while still achieving the same functional purposes for particle separation. Furthermore, this technique can be employed for the separation of specimens which are too large for current microfluidic sorting methods and are sensitive to external force fields. Such a device will greatly improve the sorting and collection processes of vulnerable biological species, such as EBs, for further downstream studies and provide ES cell researchers with healthy and homogenous populations of cells.

## Acknowledgements

This work was funded by the following agencies: National Institutes of Health (NIH) through the Roadmap for Nanomedicine Research (PN2EY018228) and NASA National Space Biomedical Research Institute (NSBRI) (NCC 9-58-317). The authors thank Dr T. S. Wong and Dr E. P. Lillehoj for their useful comments in reviewing the manuscript.

## References

1 M. Bibel, J. Richter, K. Schrenk, K. L. Tuker, V. Staiger, M. Korte, M. Goetz and Y.-A. Barde, *Nat. Neurosci.*, 2004, **7**, 1003.
2 V. Gouon-Evans, L. Boussemart, P. Gadue, D. Nierhoff, C. I. Koehler, A. Kubo, D. A. Shafritz and G. Keller, *Nat. Biotechnol.*, 2006, **24**, 1402.
3 N. Lumelsky, O. Blondel, P. Laeng, I. Velasco, R. Ravin and R. McKay, *Science*, 2001, **292**, 1389.
4 G. Keller, *Genes Dev.*, 2005, **19**, 1129.
5 G. Keller, *Curr. Opin. Cell Biol.*, 1995, **7**, 862.
6 H. Kurosawa, *J. Biosci. Bioeng.*, 2007, **103**, 389.
7 B. Valamehr, S. J. Jonas, J. Polleux, R. Wiao, S. Guo, E. H. Gschweng, B. Stiles, K. Kam, T.-J. M. Luo, O. N. Witte, X. Liu, B. Dunn and H. Wu, *Proc. Natl. Acad. Sci. U. S. A.*, 2008, **105**, 14459.

8 R. A. Marklein and J. A. Burdick, *Adv. Mater.*, 2010, **22**, 175.
9 J. Voldman, *Annu. Rev. Biomed. Eng.*, 2006, **8**, 425.
10 N. Pamme, *Lab Chip*, 2007, **7**, 1644.
11 M. Radisic, R. K. Lyer and S. K. Murthy, *Int. J. Nanomed.*, 2006, **1**, 3.
12 H. Tsutsui and C. M. Ho, *Mech. Res. Commun.*, 2009, **36**, 92.
13 D. Huh, J. H. Bahng, Y. B. Ling, H. H. Wei, O. D. Kripfgans, J. B. Fowlkes, J. B. Grotberg and S. Takayama, *Anal. Chem.*, 2007, **79**, 1369.
14 M. Madou, J. Zoval, G. Jia, H. Kido, J. Kim and N. Kim, *Annu. Rev. Biomed. Eng.*, 2006, **8**, 601.
15 J. Kruger, K. Singh, A. O'Neill, C. Jackson, A. Morrison and P. O'Brien, *J. Micromech. Microeng.*, 2002, **12**, 486.
16 A. Wolff, I. R. Perch-Nielsen, U. D. Larsen, P. Friss, G. Goranovic, C. R. Poulsen, J. P. Kutter and P. Telleman, *Lab Chip*, 2003, **3**, 22.
17 L. Huang, E. C. Cox, R. H. Austin and J. C. Sturm, *Science*, 2004, **304**, 987.
18 D. W. Inglis, J. A. Davis, R. H. Austin and J. C. Sturm, *Lab Chip*, 2006, **6**, 655.
19 M. Yamada, M. Nakashima and M. Seki, *Anal. Chem.*, 2004, **76**, 5465.
20 J. Takagi, M. Yamada, M. Yasuda and M. Seki, *Lab Chip*, 2005, **5**, 778.
21 M. Yamada and M. Seki, *Anal. Chem.*, 2006, **78**, 1357.
22 C.-F. Chou, O. Bakajin, S. W. P. Turner, T. A. J. Duke, S. S. Chan, E. C. Cox, H. G. Craighead and R. H. Austin, *Proc. Natl. Acad. Sci. U. S. A.*, 1999, **96**, 13762.
23 X. L. Zhang, J. M. Cooper, P. B. Monaghan and S. J. Haswell, *Lab Chip*, 2006, **6**, 561.
24 S. Choi and J.-K. Park, *Lab Chip*, 2007, **7**, 890.
25 J. M. Karp, J. Yeh, G. Eng, J. Fukuda, J. Blumling, K.-Y. Suh, J. Cheng, A. Mahdavi, J. Borenstein, R. Langer and A. Khademhosseini, *Lab Chip*, 2007, **7**, 786.
26 Y. Torisawa, B. Chueh, D. Huh, P. Ramamurthy, T. M. Roth, K. F. Barald and S. Takayama, *Lab Chip*, 2007, **7**, 770.
27 C. M. Cameron, W. S. Hu and D. S. Kaufman, *Biotechnol. Bioeng.*, 2006, **94**, 938.




 